

# Temperature-Dependent Synthesis of $\text{Ca}_3\text{Ni}_2\text{Fe}_{24}\text{O}_{41}$ Nano-Hexaferrite Via Oxalate-Assisted Ceramic Method

**\*Dr. Suhasini Dafe<sup>1</sup>, Dr. Raju Belekar<sup>2</sup>**

<sup>1</sup>Assistant Professor, Dept. of Physics, School of Engineering and Technology, G H Raisoni University Saikheda, Pandhurna (MP) India-480 337.

<sup>2</sup>Assistant Professor, Dept. of Physics, Institute of Science, Nagpur (MH) India-440 001.  
Corresponding Author: [suhasinidafe1983@gmail.com](mailto:suhasinidafe1983@gmail.com)

## Abstract

$\text{Ca}_3\text{Ni}_2\text{Fe}_{24}\text{O}_{41}$  nano Z-type hexaferrite was synthesized via an oxalate assisted ceramic route and sintered at 600°C and 800°C to study structural, morphological, and magnetic effects. XRD confirmed Z phase formation at both temperatures, with the 800°C sample showing enhanced crystallinity and larger crystallites. SEM showed 90-100 nm hexagonal grains at 600°C. At 800°C, grains grew to 200–370 nm, became well-interconnected, and porosity was reduced, indicating enhanced grain-boundary diffusion and densification. Magnetic measurements showed slight reductions in coercivity, saturation magnetization, and retentivity at the higher temperature, aligning with grain-growth behavior reported in the literature. The 800°C sintering condition achieved optimal structural uniformity and soft magnetic traits, making it a strong candidate for high-frequency devices and EMI-shielding applications.

**Keywords:** Z-type, Nano-hexaferrite, Ceramic, Temperature, Coercivity

## Introduction:

Z-type Hexaferrites have a significant attention due to their adaptable properties like thermal stability magnetic properties and high electrical resistivity, essential for microwave and high-frequency applications [1, 2]. The unique ferrimagnetic behaviour of these materials, is due to the complex superexchange interactions between  $\text{Fe}^{3+}$  ions occupying multiple crystallographic sites [3]. Their magnetic properties are highly dependent on the distribution of these ions inside the crystal structure. The nickel-substituted Z-type hexaferrites hold significant importance due to their refined magnetocrystalline anisotropy and enhanced magnetic softness [4]. In former years, scientist shifted their research from bulk to nano hexaferrites, which are now being utilized across a wide range of applications.

The structural and magnetic properties of hexaferrites are strongly influenced by synthesis method and sintering temperature. The conventional ceramic method, with an oxalate precursor, provide a scalable synthesis and cost-effective route with improving reaction kinetics and precursor homogeneity at relatively lower sintering temperatures [5,6]. Introduction of oxalate into the ceramic synthesis method, leads to achieved better diffusion

between metal ions and fine particle formation, thereby enhancing phase purity and controlling grain growth [7].

This study emphasizes the temperature-dependent study of  $\text{Ca}_3\text{Ni}_2\text{Fe}_{24}\text{O}_{41}$  nano-hexaferrite at 600°C and 800°C via oxalate- aided ceramic method. Ample characterization techniques including X-ray Diffraction (XRD), Scanning Electron Microscopy (SEM) and B-H curve study for structural analysis, morphological investigation, and for magnetic behavior are studied to evaluate the phase purity, morphology, and magnetic behavior of the material. The primary goal of the investigation is to identify the optimal sintering conditions that gives desired structural and magnetic characteristics suitable for potential applications in high-frequency transformers, microwave devices and magnetic sensors.

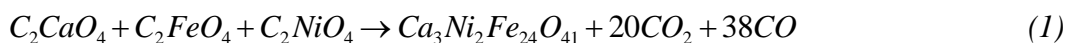
## **Methodology**

### **Material Selection:**

Nickel-containing hexaferrites were usually identified for their high magnetic permeability, low core losses with brilliant performance in high-frequency applications. For this study,  $\text{Ni}^{2+}$  was chosen due to its noble magnetic properties, while calcium and iron preferred as the primary components of the  $\text{Ca}_3\text{Ni}_2\text{Fe}_{24}\text{O}_{41}$  Z-type hexaferrite.

### **Synthesis Method:**

The  $\text{Ca}_3\text{Ni}_2\text{Fe}_{24}\text{O}_{41}$  Z-type hexaferrite was synthesized using conventional ceramic method integrating an oxalate precursor route to improve uniformity and reactivity. Stoichiometric amounts of iron oxalate ( $\text{C}_2\text{FeO}_4$ ), calcium oxalate ( $\text{C}_2\text{CaO}_4$ ), and nickel oxalate ( $\text{C}_2\text{NiO}_4$ ) were precisely weighed and properly blended using an agate mortar to get a homogeneous mixture according to equation (1).



### **Calcination and Sintering:**

The prepared mixture was sintered at two different temperatures of 600°C and 800°C to study the influence of temperature on phase formation and magnetic properties. These samples were sintered for 12 hours in a muffle furnace at atmospheric conditions for proper crystallization as well grain growth.

### **Characterization Techniques:**

- Crystal structure and phase purity was examined by X-ray Diffraction (XRD) study
- Particle morphology and surface texture was studied by Scanning Electron Microscopy (SEM).
- Magnetic parameters such as saturation magnetization (Ms), coercivity (Hc), and remanent magnetization (Mr) were analysed via BH curve.

## **Results and discussion:**

## X-ray Diffraction

X-ray powder diffraction (XRD) was used to study the crystalline phases and structural characteristics of  $\text{Ca}_3\text{Ni}_2\text{Fe}_{24}\text{O}_{41}$  nano-hexaferrites synthesized by the conventional ceramic method incorporating an oxalate precursor route. The diffraction patterns of samples sintered at 600°C and 800°C were recorded using Cu-K $\alpha$  radiation ( $\lambda = 1.5406 \text{ \AA}$ ) and are shown in Figure 1. The comparison of obtained diffraction patterns with the standard JCPDS database is executed to confirming the phase formation.

The existence of distinctive low-angle diffraction peaks around 10.3° and 12.1°, which correspond to the (003) and (006) planes, respectively, indicated the beginning of the production of the Z-type hexaferrite phase at 600°C. These broad, lower-intensity peaks, however, suggested inadequate phase development, tiny crystallite size, and poor crystallinity. There were further, less distinct peaks at 21.2° (101), 24.2° (102), 30.1° (110), 33.2° (114), and 35.3° (200). These characteristics point to the potential occurrence of intermediate or amorphous phases, partial breakdown of the precursor, and the existence of nano-crystalline domains. The Z-type phase's early-stage development around 600 °C is consistent with the kinetic constraints that prevent long-range structural ordering from being achieved at comparatively lower temperatures.

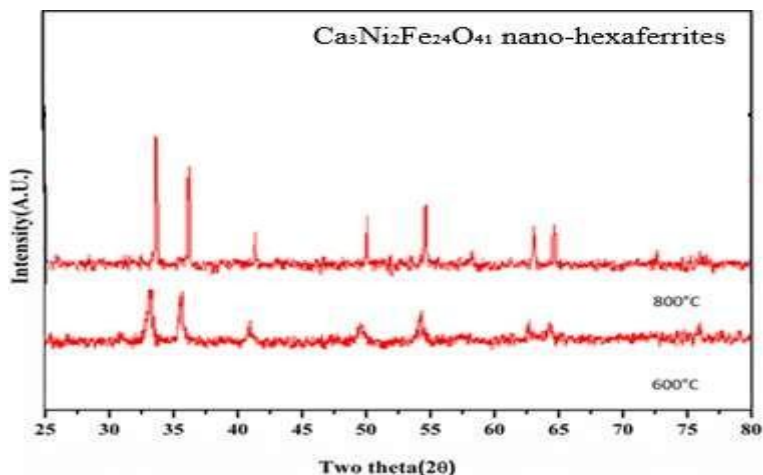
The sample sintered at 800°C, on the other hand, exhibits a significant change in structural characteristics in its XRD pattern. A single-phase Z-type hexaferrite was confirmed to have formed when all of the distinctive peaks of Z-type hexaferrite matched those reported in JCPDS 19-0097. Being the characteristic of Z-type hexaferrites, the low-angle (003) and (006) reflections at ~10.3° and ~12.1° sharpened and intensified, revealing a well-developed layered hexagonal structure. There were also further conspicuous high-intensity peaks at 30.1° (110), 33.2° (114), 35.3° (200), 37.2° (203), and 41.5° (206) that confirmed full crystallization and phase purity. Improved long-range order and the completion of solid-state processes were indicated by the appearance of minor peaks in the 800°C pattern at 45.8° (210) and 52.3° (217), which were not present in the 600°C sample.

The crystallite size grew dramatically from about 27.8 nm (600 °C) to 43.2 nm (800 °C), as determined using the Debye-Scherrer equation. This expansion is a result of increased thermal energy at higher sintering temperatures, which encourages grain coarsening and lowers lattice strain.

In addition, the lattice parameters were calculated on the assumption of a hexagonal crystal system (space group  $\text{P6}_3/\text{mmc}$ ) utilizing Bragg's law and indexed peaks. The computed lattice constants for the 600°C sample were  $a = 5.87 \text{ \AA}$  and  $c \approx 52.5 \text{ \AA}$ . These numbers marginally rose to  $a = 5.91 \text{ \AA}$  and  $c \approx 52.8 \text{ \AA}$  at 800 °C, which is explained by better crystallographic alignment during sintering. Standard Z-type ferrites described in the literature are also compatible with these lattice parameter values.

The comparative analysis shows that 800°C is a more favorable temperature for the full development of the Z-type hexaferrite phase, which includes correct lattice formation, increased crystallinity, and larger crystallite size. This enhancement is necessary for Z-type

hexaferrites' possible uses in high-frequency devices, electromagnetic wave absorbers, and space communication materials—all of which depend on structural stability and well-defined magnetic anisotropy.



Figures 1: XRD pattern of  $\text{Ca}_3\text{Ni}_2\text{Fe}_{24}\text{O}_{41}$  nano-hexaferrites synthesized at 600°C and 800°C

### Scanning Electron Microscopy (SEM)

Scanning Electron Microscopy (SEM) was used to examine the surface morphology of  $\text{Ca}_3\text{Ni}_2\text{Fe}_{24}\text{O}_{41}$  nano-hexaferrite samples prepared via the oxalate-assisted ceramic method and sintered at 600°C and 800°C. Figures 2 and 3 show the SEM micrographs of the samples annealed at 600°C and 800°C, respectively.

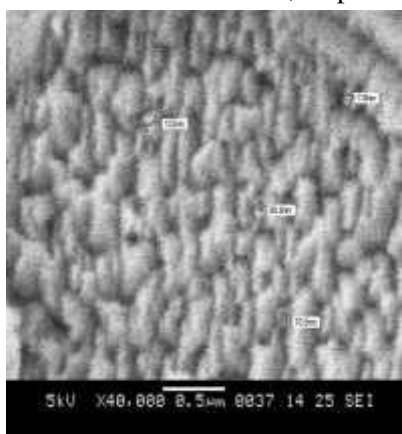


Figure 2: SEM images of the sample prepared at 600°C.

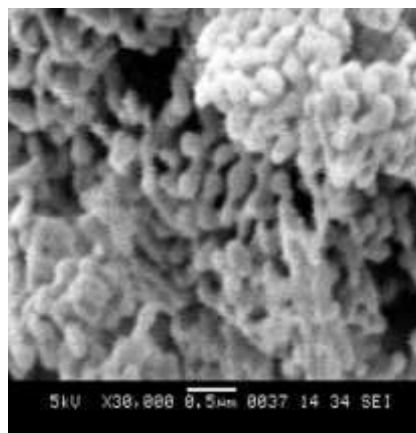


Figure 3: SEM images of the sample prepared at 800°C.

$\text{Ca}_3\text{Ni}_2\text{Fe}_{24}\text{O}_{41}$  hexaferrite SEM images show that at 600 °C, the microstructure consists of densely packed clusters of distinct hexagonal plate-like grains with moderate porosity, which

is typical of early-stage ferrite formation and sintering limited by surface diffusion. Individual particle sizes average 90 to 100 nm. The microstructure exhibits obvious grain development and densification upon sintering at 800 °C, with faceted, hexagonal grains expanding to a range of 200–370 nm. (8–10).

Sharper XRD reflections in the 800°C sample demonstrate enhanced crystallinity, which confirms the integrity of the Z-type lattice and parallels this structural progression. Grain-size-dependent magnetic trends in ferrites are consistent with the coarser, denser grains at 800°C, which promote multi-domain behavior, reduce coercivity, and slightly increase saturation magnetization due to decreased surface-spin disorder. The finer grains at 600°C, on the other hand, support domain-wall pinning, which results in higher coercivity (7, 1–13).

Overall, the 800°C sintering temperature strikes the ideal equilibrium, creating a uniform, crystalline, well-bonded hexagonal microstructure that improves  $\text{Ca}_3\text{Ni}_2\text{Fe}_{24}\text{O}_{41}$  's structural and magnetic performance and qualifies it for high-frequency and microwave applications.

### Magnetic Properties (B–H Curve Analysis)

Using a hysteresis loop tracer, the magnetic behavior of  $\text{Ca}_3\text{Ni}_2\text{Fe}_{24}\text{O}_{41}$  nano-hexaferrite samples sintered at 600°C and 800°C was examined. The B-H loops plotted for each sample were used to calculate the three primary magnetic parameters: retentivity ( $M_r$ ), saturation magnetization ( $M_s$ ), and coercivity ( $H_c$ ). Understanding the material's suitability for high-frequency and microwave applications depends on these tests.

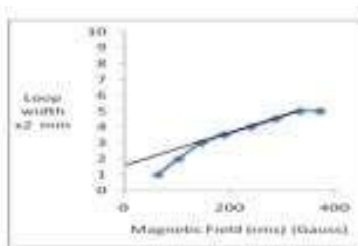


Figure a: Dependence of loop width on magnetic field

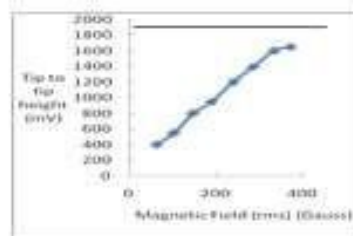


Figure b: Dependence of twice the intercept on magnetic field

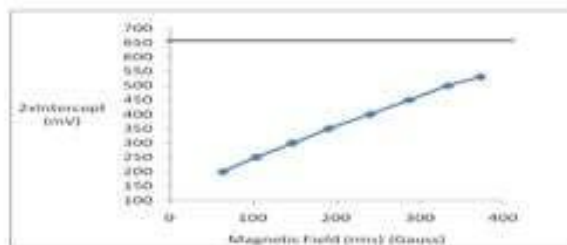


Figure c: Dependence of tip to tip separation on magnetic field

Figure 4: Graph of the sample prepared at 600°C temperature.

For both  $\text{Ca}_3\text{Ni}_2\text{Fe}_{24}\text{O}_{41}$  hexaferrite samples, the B–H tests show low hysteresis loops, indicating their soft magnetic nature appropriate for high-frequency applications. Coercivity, saturation magnetization, and retentivity all marginally decrease when the sintering temperature rises from 600°C to 800°C. This phenomenon is consistent with well-established magnetic theory, which states that as grain size increases, domain-wall pinning decreases, making it simpler for magnetic domains to migrate and reducing coercivity and saturation magnetization [8, 11–13]. Retentivity only slightly decreases, indicating that despite microstructural alterations, zero-field domain alignment is essentially stable.

Clear, hexagonal plate-like grains (~90–100 nm) form densely agglomerated clusters at 600 °C, according to SEM studies. This suggests significant surface energy and magnetic interaction during low-temperature sintering. Although the grains coarsen to around 200–370 nm when sintered at 800 °C, their faceted hexagonal form is retained. Increased diffusion and grain-boundary mobility due to the higher temperature lead to neck development, decreased porosity, and a compact, interconnected microstructure, which are characteristics of intermediate-stage sintering [8–10]. Sharper XRD peaks confirm better crystallinity and support this densification. The evolution of microstructure has a direct impact on magnetic behavior: the larger grains at 800°C support multi-domain structures, which reduce coercivity and slightly increase magnetization due to reduced surface-spin disorder, while the smaller grains at 600°C facilitate domain-wall pinning and, therefore, higher coercivity (7, 13–16).

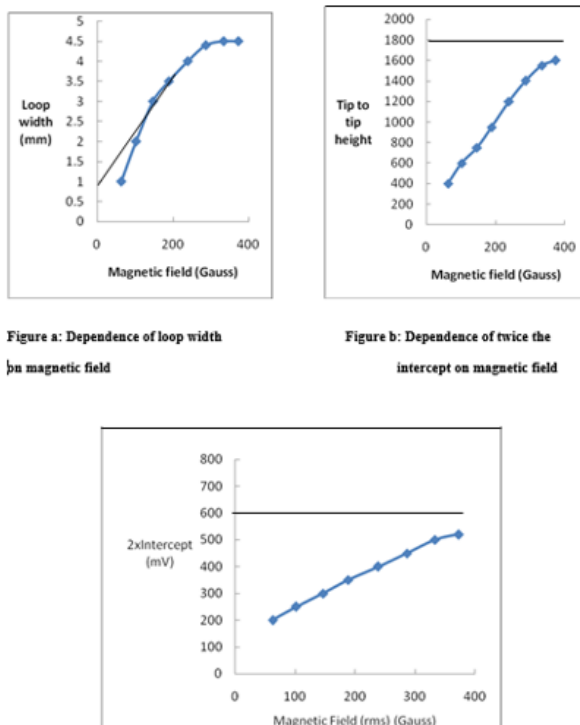


Figure 5: Graph of the sample prepared at 800°C temperature.

With a balanced microstructural and magnetic profile, 800°C sintering produces a compact, crystalline hexagonal shape with soft magnetic qualities, making it the ideal temperature for high-frequency and microwave device applications.

### Conclusion:

In this study,  $\text{Ca}_3\text{Ni}_2\text{Fe}_{24}\text{O}_{41}$  nano Z-type hexaferrite was synthesized via an oxalate-assisted ceramic route and sintered at 600 °C and 800 °C to examine effects on structure, morphology, and magnetism. XRD confirmed Z-phase formation at both temperatures, with the 800 °C sample showing improved crystallinity and larger crystallite size. SEM revealed that the 600 °C sample consisted of dense clusters of ~90–100 nm hexagonal grains, while the 800 °C sample featured much larger (~200–370 nm), well-connected hexagonal grains with reduced porosity, indicating enhanced diffusion and grain-boundary mobility. B–H loop analysis showed modest reductions in coercivity, saturation magnetization, and retentivity at higher temperatures, attributed to grain growth reducing domain-wall pinning. Overall, 800 °C sintering optimized structural uniformity and magnetic softness, making it ideal for high-frequency and EMI-shielding applications.

### References

1. Pullar, R. C. (2012). Hexagonal ferrites: A review of the synthesis, properties and applications of hexaferrite ceramics. *Progress in Materials Science*, 57(7), 1191–1334. <https://doi.org/10.1016/j.pmatsci.2012.04.001>
2. Ghasemi, A., Shirsath, S. E., & Morisako, A. (2011). Structural and magnetic properties of Z-type  $\text{Sr}_3\text{Co}_2\text{Fe}_{24}\text{O}_{41}$  hexaferrite nanoparticles prepared by sol–gel auto-combustion method. *Journal of Alloys and Compounds*, 509(5), 1979–1983. <https://doi.org/10.1016/j.jallcom.2010.10.187>
3. Sugimoto, M. (1999). The past, present, and future of ferrites. *Journal of the American Ceramic Society*, 82(2), 269–280. <https://doi.org/10.1111/j.1151-2916.1999.tb01840.x>
4. Gul, I. H., & Ahmad, F. (2008). Effect of Ni substitution on structural and magnetic properties of Ca-Z-type hexaferrites prepared by coprecipitation method. *Journal of Magnetism and Magnetic Materials*, 320(3–4), 330–333. <https://doi.org/10.1016/j.jmmm.2007.06.004>
5. Patange, S. M., Shirsath, S. E., & Jadhav, K. M. (2008). Effect of annealing temperature on structural and magnetic properties of Co-Zn ferrite prepared by oxalate co-precipitation method. *Materials Chemistry and Physics*, 109(2–3), 393–398. <https://doi.org/10.1016/j.matchemphys.2007.11.036>
6. Vijaya Kumar, K., Rao, G. V. S., & Prasad, S. C. (2005). Preparation and characterization of calcium ferrite by oxalate precursor route. *Materials Research Bulletin*, 40(8), 1353–1362. <https://doi.org/10.1016/j.materresbull.2005.04.007>
7. Shirsath, S. E., et al. (2013). Influence of synthesis routes on structural and magnetic properties of nanocrystalline spinel ferrites: A review. *Journal of Magnetism and Magnetic Materials*, 349, 208–215. <https://doi.org/10.1016/j.jmmm.2013.08.001>
8. Hajalilou, H., et al. (2015). Effects of milling atmosphere and increasing sintering temperature on the magnetic properties of nanocrystalline  $\text{Ni}_{0.36}\text{Zn}_{0.64}\text{Fe}_2\text{O}_4$ . *Journal of Nanomaterials*, Article ID 615739.
9. Azis, R. S., Mustaffa, M. S., & Shahrani, N. M. (2018). Sintering Temperature Effect on Microstructure and Magnetic Evolution Properties with Nano- and Micrometer Grain Size in Ferrite Polycrystals. In *Sintering Technology – Method and Application*. IntechOpen. <https://doi.org/10.5772/intechopen.78638>
10. Low, Z. H., Ismail, I., & Tan, K. S. (2018). Sintering Processing of Complex Magnetic Ceramic Oxides: A Comparison Between Sintering of Bottom-Up Approach Synthesis and Mechanochemical Process of Top-Down Approach Synthesis. In M. Liu (Ed.), *Sintering Technology – Method and Application* (pp. 25–43). IntechOpen. <https://doi.org/10.5772/intechopen.78654>
11. Chagas, E. F., Ponce, A. S., Prado, R. J., Silva, G. M., Bettini, J., & Baggio-Saitovitch, E. (2014). Thermal effect on magnetic parameters of high-coercivity cobalt ferrite. *Journal of Applied Physics*, 116(3).
12. Mahmood, S.H., Al Sheyab, Q., Bsoul, I., Mohsen, O. and Awadallah, A., 2018. Structural and magnetic properties of Ga-substituted  $\text{Co}_2\text{W}$  hexaferrites. *Current Applied Physics*, 18(5), pp.590-598.
13. Fang, Z.Z. and Wang, H., 2008. Densification and grain growth during sintering of nanosized particles. *International Materials Reviews*, 53(6), pp.326-352.



14. Rana, M. U., & Abbas, T. "The effect of Zn substitution on microstructure and magnetic properties of  $\text{Cu}_{1-x}\text{Zn}_x\text{Fe}_2\text{O}_4$  ferrite." *Journal of Magnetism and Magnetic Materials*, 246(1–2), 110–114 (2002). [https://doi.org/10.1016/S0304-8853\(02\)00037-9](https://doi.org/10.1016/S0304-8853(02)00037-9)
15. Pan, W., Gu, F., Qi, K., Liu, Q., & Wang, J. "Effect of Zn substitution on morphology and magnetic properties of copper ferrite nanofibers." *arXiv* (2011).
16. Dafe, S., & Salunkhe, M. "Effect Of Diamagnetic Mg Substitution on Structural and Magnetic Properties of  $\text{Ni}_2\text{Z}$  Hexaferrite." *International Journal of Scientific Research and Engineering Studies (IJSRES)*, 2(10) (2015).